Chemical Science

ROYAL SOCIETY OF CHEMISTRY

EDGE ARTICLE

View Article Online
View Journal | View Issue

Cite this: *Chem. Sci.*, 2022, **13**, 8321

All publication charges for this article have been paid for by the Royal Society of Chemistry

NHC induced radical formation *via* homolytic cleavage of B–B bonds and its role in organic reactions†

Laura Kuehn,[a] Ludwig Zapf,[a] Luis Werner,[a] Martin Stang, ‡[a] Sabrina Würtemberger-Pietsch,[a] Ivo Krummenacher,[a] Holger Braunschweig, [a] Emmanuel Lacôte, *[b] Todd B. Marder *[a] and Udo Radius *[a]

New borylation methodologies have been reported recently, wherein diboron(4) compounds apparently participate in free radical couplings *via* the homolytic cleavage of the B–B bond. We report herein that bis-NHC adducts of the type $(NHC)_2 \cdot B_2(OR)_4$, which are thermally unstable and undergo intramolecular ring expansion reactions (RER), are sources of boryl radicals of the type $NHC–BR_2^{\bullet}$, exemplified by $Me_2Im^{Me} \cdot Bneop^{\bullet}$ **1a** (Me_2Im^{Me} = 1,3,4,5-tetramethyl-imidazolin-2-ylidene, neop = neopentylglycolato), which are formed by homolytic B–B bond cleavage. Attempts to apply the boryl moiety **1a** in a metal-free borylation reaction by suppressing the RER failed. However, based on these findings, a protocol was developed using $Me_2Im^{Me} \cdot B_2pin_2$ **3** for the transition metal- and additive-free boryl transfer to substituted aryl iodides and bromides giving aryl boronate esters in good yields. Analysis of the side products and further studies concerning the reaction mechanism revealed that radicals are likely involved. An aryl radical was trapped by TEMPO, an EPR resonance, which was suggestive of a boron-based radical, was detected *in situ*, and running the reaction in styrene led to the formation of polystyrene. The isolation of a boronium cation side product, $[(Me_2Im^{Me})_2 \cdot Bpin]^+I^-$ **7**, demonstrated the fate of the second boryl moiety of B_2pin_2. Interestingly, Me_2Im^{Me} NHC reacts with aryl iodides and bromides generating radicals. A mechanism for the boryl radical transfer from $Me_2Im^{Me} \cdot B_2pin_2$ **3** to aryl iodides and bromides is proposed based on these experimental observations.

Received 12th April 2022
Accepted 7th June 2022

DOI: 10.1039/d2sc02096c

rsc.li/chemical-science

Introduction

Diboron(4) compounds are extremely useful reagents for the synthesis of organoboronates, which are valuable building blocks in organic synthesis.[1] In addition to their use in Suzuki–Miyaura crossing–coupling reactions[2] the C–B bond can easily be converted into numerous functional groups.[1] While early catalytic borylation reactions typically employed precious metal catalysts, first row "Earth abundant" transition metals have become of increasing interest, due to their low cost and low toxicity.[3,4] Recently, transition metal-free methods which activate the B–B bond of diboron(4) compounds have attracted much attention,[5] having the advantage of avoiding metal contamination in the final organic product. sp^2–sp^3 Lewis base adducts of diboron(4) compounds show a higher reactivity of the B–B bond than their respective sp^2–sp^2 precursors, due to the increased bond length and polarity. Thus, they are used in various borylation reactions or for the diboration of unsaturated substrates, in which a nucleophilic boryl moiety is generated when one of the two boron atoms is coordinated to a strong Lewis base. In 2009, Hoveyda *et al.* proposed that an NHC sp^2–sp^3 diboron(4) adduct is responsible for the metal-free β-borylation of α,β-unsaturated carbonyl compounds.[6]

Unlike heterolysis, induced by anionic nucleophiles,[5b,e] homolytic cleavage of the B–B bond is challenging due to the relatively high bond dissociation energies (BDE) of the diboron(4) compounds. For example, Wang *et al.* reported a metalfree borylation process for the direct conversion of aryl amines to aryl pinacol boronates. A radical mechanism involving single electron transfer between an aryl diazonium ion formed and a tetra-coordinated boron complex has been proposed for this reaction. Recently, new borylation

[a]*Institute for Inorganic Chemistry, Institute for Sustainable Chemistry & Catalysis with Boron, Julius-Maximilians-Universität Würzburg, Am Hubland, 97074 Würzburg, Germany. E-mail: todd.marder@uni-wuerzburg.de; u.radius@uni-wuerzburg.de*

[b]*Univ Lyon, Université Claude Bernard Lyon 1, CNRS, CNES, ArianeGroup, LHCEP, Bât. Raulin, 2 rue Victor Grignard, F-69622 Villeurbanne, France. E-mail: emmanuel.lacote@univ-lyon1.fr*

† Electronic supplementary information (ESI) available: Detailed descriptions of the experimental procedures, product characterization data, NMR spectra, screening data, and data related to the computational studies. Crystal data collection and processing parameters. CCDC 2162556 (**1**) and CCDC 2162557 (**7**). For ESI and crystallographic data in CIF or other electronic format see https://doi.org/10.1039/d2sc02096c

‡ Present Address: Department of Chemistry, University of California, Irvine, CA 92697, USA

methodologies have been reported, wherein the boron reagent apparently participates in free radical coupling *via* the homolytic cleavage of the B–B bond.[5d,8] To date, there are mainly two ways to realize this homolytic cleavage, *i.e.*, *para*-substituted pyridine-induced or by irradiation with light. Initially, the groups of Suginome and Ohmura reported the transition metal-free diboration of 1,4-dihydropyrazine derivatives and 4,4′-bipyridine, respectively, simply by reaction with B_2pin_2 at elevated temperatures.[9,10] While they initially proposed a mechanism proceeding *via* a nucleophilic pathway,[9a] their more recent reports[9b,10] confirm the role of radicals and the homolytic cleavage of the B–B bond in these processes.

In 2016, Li *et al.* reported the homolytic cleavage of the B–B bond of B_2pin_2 *via* the coordination of 4-cyanopyridine to both boron atoms, generating pyridine-stabilized boryl radicals, which were employed for the synthesis of various organoboronates.[11] Hydroboration of alkenes using B_2pin_2 and catalytic amounts of 4-cyanopyridine was demonstrated by the group of Cai, who also proposed that the reaction proceeded *via* the formation of a 4-cyanopyridine-stabilized boryl radical.[12] Jiao *et al.* described the borylation of various aryl halides using potassium methoxide in the presence of catalytic amounts of 4-phenylpyridine, proposing the *in situ* generation of super electron donors (SED) based on boryl-pyridine species.[13] In contrast to the initial assumption of a homolytic B–B bond cleavage,[13a] DFT studies demonstrate that the SEDs are generated by heterolytic cleavage of the B–B bond in B_2pin_2 *via* coordination of the two boron atoms by pyridine and methoxide, respectively.[13b] In 2017, the groups of Pinet and Pucheault reported the stoichiometric borylation of various aryl iodides, mediated by an *in situ* formed fluoride sp^2–sp^3 diboron adduct from B_2pin_2 and CsF. This anionic adduct, previously structurally characterized by our group,[5b] was proposed to reduce the aryl iodide *via* a single-electron-transfer process (SET), forming FBpin[5e] and a boryl radical, which is stabilized by pyridine.[14] Furthermore, a decarboxylative borylation of aryl and alkenyl carboxylic acids *via* a radical coupling mechanism was reported by Fu and co-workers.[15] An *in situ* formed three-component bis-adduct between B_2pin_2, the carboxylic acid substrate, and a pyridine derivative is assumed to undergo homolytic B–B bond cleavage by an intramolecular SET, generating a carboxylate radical and a pyridine-stabilized boryl radical.[15] Ogawa *et al.* reported the diboration of terminal alkynes with B_2pin_2 under irradiation by a high pressure mercury lamp in the presence of catalytic amounts of diphenyl disulfide and triphenylphosphine giving 1,2-diborylalkenes.[16] The mechanism is not yet clear, but boron-centered radicals are proposed to be formed from B_2pin_2 and PPh_3 under irradiation.[16b] In 2018, Studer and co-workers introduced the radical borylation of alkyl and aryl iodides initiated by a photoinduced C–I bond homolysis.[17a] The alkyl/aryl radical formed presumably adds to B_2cat_2 and, with coordination of DMF (dimethylformamide), the weakened B–B bond homolyzes giving the alkyl/aryl boronic ester and a DMF-stabilized boryl radical.[17] Just recently, the photocatalytic, regioselective radical borylation of α,β-unsaturated esters and related compounds has been reported,[18] and we reported the transition metal-free borylation of primary and secondary alkyl sulfones to yield alkylboronic esters.[19] For the latter, the reaction of alkyl sulfones with bis(neopentyl glycolato) diboron(4) (B_2neop_2) and a stoichiometric amount of base as promotor afforded alkylboronic esters with a wide functional group tolerance. Radical clock, radical trap experiments, and EPR studies revealed that the borylation process involves radical intermediates.[19]

Typical methods for increasing the lifetime of radical species involve delocalization of the unpaired electron and/or the use of sterically hindered groups to prevent dimerization.[8c,20] With respect to boron-centered radicals, well known anionic species of the type $BR_3^{\bullet-}$ are generated by occupying the vacant p-orbital of an electron deficient borane with a single electron.[21] For example, our group recently reported a structurally characterized example, in which such a radical anion is stabilized by an *ortho*-carborane moiety.[21i] In contrast, neutral analogs result from coordination of a Lewis base (L) to the boron center giving an $L–BR_2^{\bullet}$ adduct. In recent years, the electrophilicity of *N*-heterocyclic carbenes (NHCs) has been employed for stabilizing such boron centered radicals (Scheme 1).[22] Offering an empty π*-orbital, the NHC is able to engage in π-backbonding interactions and thus delocalize the unpaired electron, which lowers the bond dissociation energies of the corresponding boranes.[20,22,23]

The groups of Curran, Lacôte, and Lalevée have extensively studied NHC-stabilized radicals of the type $NHC–BH_2^{\bullet}$ **A**, which are formed from the borane adduct $NHC\cdot BH_3$ by homolytic B–H bond cleavage. Radical formation from $NHC\cdot BH_3$ is facilitated by the relatively small homolytic B–H bond dissociation energy (80–88 kcal mol^{-1})[24] in the precursor induced by the increased spin delocalization in the resulting ligated radical.[25] This bond cleavage can be realized in the presence of radical initiators such as DTBP (di-*tert*-butylperoxide) or azobisisobutyronitrile (AIBN), triggered by light or heat. However, these radicals are transient and cannot be isolated. EPR studies and corroborating theoretical data reveal that radicals of type **A** are planar with the spin density delocalized over the NHC ligand and the boron center.[24] This class of compounds has been applied as efficient co-initiators in radical photopolymerization reactions as well as radical reductions of halides and xanthates.[26] The same groups generated the corresponding aryl boron radicals by analogously abstracting hydrogen atoms from $NHC\cdot BH_2Ar$ compounds *via* homolytic B–H bond cleavage.[26h] The groups of Curran, Taniguchi, and Wang achieved various borylative radical cyclization reactions and the borylation of polyfluoroarenes, as well as the radical hydroboration of alkenes, also utilizing $NHC\cdot BH_3$ with *in situ* formation of the NHC-boryl radical **A** (Scheme 1) by hydrogen atom abstraction using di-*tert*-butyl hyponitrile and AIBN, respectively.[27,28]

The acridinyl radical **B**, reported by Gabbaï *et al.* in 2007, can be considered as the first structurally characterized carbene-stabilized neutral boryl radical (Scheme 1).[29] However, in this example, the unpaired electron is largely delocalized over the acridinyl fragment with very little contribution from the boron atom, as indicated by EPR spectroscopy. The same group observed, but could not isolate, radical **C** by introducing a nucleophilic NHC (Scheme 1), *via* reversible reduction of an

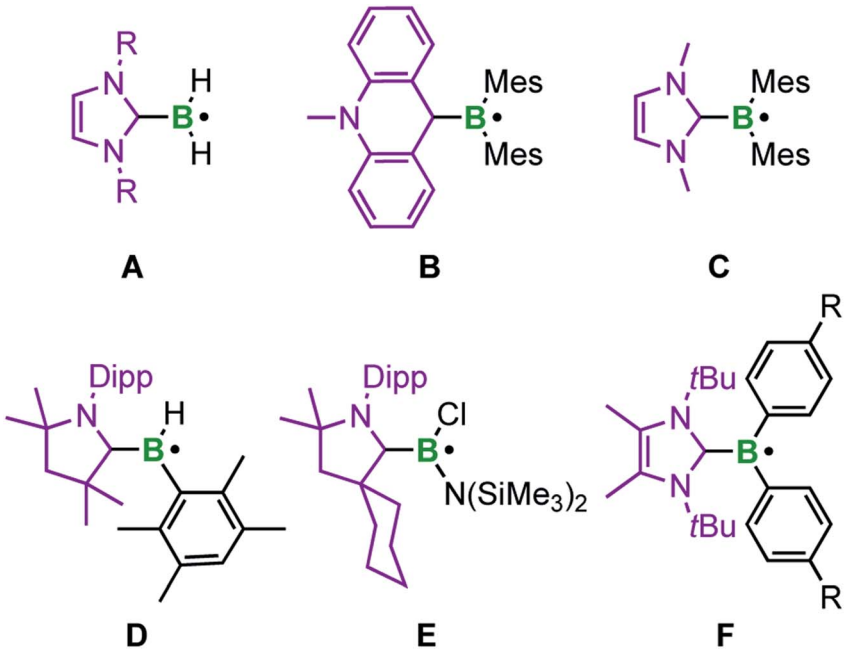

Scheme 1 Selected neutral boryl radicals stabilized by carbenes.

NHC-stabilized borenium cation.[30] Radical **C** reveals a higher boron radical character and significant localization of the unpaired electron in a (B–C_{NHC})π-orbital.[30] In 2014, Braunschweig and co-workers isolated the $cAAC^{Me}$-stabilized (cAAC = cyclic alkyl amino carbene) boryl radical **D** by reduction of the corresponding haloborane adduct.[31] EPR and DFT data indicate that the spin density is delocalized over the strong π-accepting cAAC ligand. In the same year, the similar $cAAC^{Cy}$-stabilized aminoboryl radical **E**, generated analogously by reduction of the corresponding adduct, was introduced by the groups of Bertrand and Stephan.[32] Recently, Tamm *et al.* reported the NHC-stabilized boryl radical **F**, prepared by reduction of the corresponding borenium cation. Radical **F** was structurally confirmed and characterized by EPR spectroscopy, revealing that the unpaired electron is almost exclusively localized on the $B(Ar)_2$ moiety.[33] In general, NHCs, and especially cAACs, provide significant stabilization of boron-based radicals, with NHCs being at a unique cross-road between stabilization and reactivity, which has led to the strong focus discussed above.

For many years, our groups have been intensively studying neutral pyridine[34] and NHC[6c,35] as well as anionic[5b] adducts[5a,36] of diboron(4) compounds.[1b] We have shown that, depending on the stoichiometry and the steric demand of the NHC and the diboron(4) reagent, mono- or bis-NHC adducts are accessible.[35] In the current paper we focus on how NHC complexation of diboron(4) derivatives can be harnessed for radical reactions, beyond ring expansion reactions (RER).

Results and discussion

The RER of bis-NHC adducts typically proceeds *via* the insertion of one $B(OR)_2$ moiety into the C–N bond of one NHC.[35] A second *exo*-$B(OR)_2$ moiety binds to the former carbene–carbon atom. In the case of B_2neop_2 (neop = neopentylglycolato), the endocyclic Bneop ring opens and one oxygen atom binds to the exocyclic boron atom forming an 8-membered heterocyclic ring with the second NHC coordinated to the endocyclic boron atom (Scheme 2).

For B_2neop_2 this RER occurs at room temperature, whereas for B_2cat_2 (cat = catecholato) elevated temperatures of 70 °C are required.[35a] For small NHCs (*e.g.* Me_2Im^{Me} or $^iPr_2Im$) and the small diboron(4) reagent B_2eg_2 (eg = ethyleneglycolato), RERs are observed at temperatures as low as −40 °C.[35c] Furthermore, we have shown that the reactivity at diboron(4) compounds also depends on the NHC. For example, the reaction of B_2cat_2 with $Dipp_2Im$ (unsaturated NHC backbone) and $Dipp_2Sim$ (saturated NHC backbone) leads, in both cases, to the mono-NHC adduct. However, whereas $Dipp_2Im{\cdot}B_2cat_2$ is stable with regard to RER, the adduct with the backbone-saturated NHC $Dipp_2Sim{\cdot}B_2cat_2$ is thermally unstable generating a ring-expansion product.[35c]

Based on the above findings, we were interested to obtain further insight into the subsequent reactivity of bis-NHC adducts of diboron(4) compounds as well as the mechanism of the RERs. As the RER is very fast, and we could not exclude a mechanism involving radicals, we began our studies by monitoring the RER of B_2neop_2 with two equivalents of Me_2Im^{Me} in THF by EPR spectroscopy (Fig. 1). Beginning at −80 °C, we slowly raised the temperature, as our previous studies have shown that, at room temperature, the ring-expanded product RER-$(Me_2Im^{Me})_2{\cdot}B_2neop_2$ **2** is quantitatively generated within minutes.

At 290 K, a weak multiline EPR signal was detected with an isotropic *g*-value of 2.003 (Fig. 1). With the anticipated formation of a radical of the type NHC-$BR_2^{\bullet}$ (Me_2Im^{Me}-Bneop$^{\bullet}$) **1a**, presumably generated by homolytic cleavage of the B–B bond in

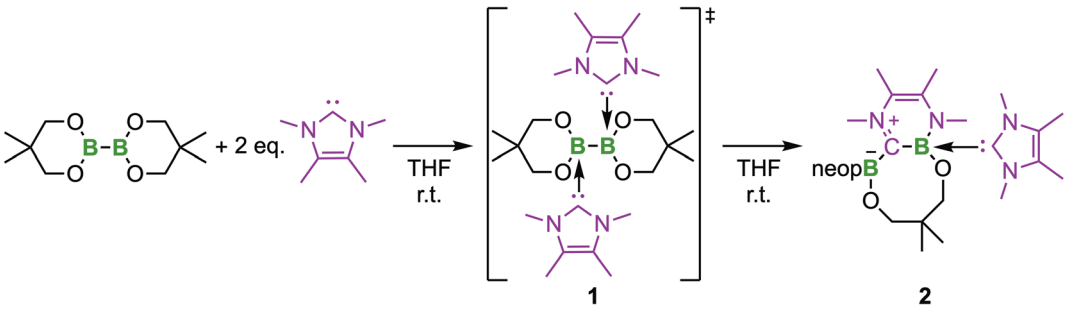

Scheme 2 Reaction of B_2neop_2 with two equivalents of Me_2Im^{Me} at room temperature forming the ring expanded product RER-B_2neop_2-$\cdot(Me_2Im^{Me})_2$ **2** with the bis-NHC adduct $(Me_2Im^{Me})_2\cdot B_2neop_2$ **1** as an intermediate.

B_2neop_2, spectral fitting (Fig. 1, red) suggests a delocalized spin distribution over the NHC fragment with hyperfine couplings to boron ($a(^{11}B) = 8.7$ MHz), to nitrogen ($a(^{14}N) = 9.5$ MHz), and to the methyl protons of the NHC ($a(^{1}H) = 6.9$ and 7.9 MHz). Bis-NHC adducts, such as $(Me_2Im^{Me})_2\cdot B_2neop_2$ **1**, with both boron atoms coordinated by an NHC, reveal an increased bond length and therefore a weakened boron–boron bond. X-ray diffraction of single crystals of $(Me_2Im^{Me})_2\cdot B_2neop_2$ **1**, obtained from a saturated solution of B_2neop_2 and two equivalents of Me_2Im^{Me} in toluene at −30 °C (Fig. 2a) revealed, that both boron atoms of **1** are sp^3-hybridized and tetrahedrally coordinated with a B–B bond distance of 1.770(2) Å, significantly elongated compared to that observed for B_2neop_2 (1.712(3) Å).[35c] According to DFT calculations (M06-2x//def2-TZVPP(B)/def2-TZVP), the dissociation energies of the B–B bonds in the diboron(4) compounds drop significantly upon NHC coordination to boron, from 408.9 kJ mol^{-1} for B_2neop_2 to 254.7 kJ mol^{-1} for $(Me_2Im)\cdot B_2neop_2$ to 105.5 kJ mol^{-1} for $(Me_2Im)_2\cdot B_2neop_2$ (Fig. 2c). The reason for this weakening lies in the stabilization of the resulting boryl radicals by delocalization on the NHC. The decrasing B–B bond strengths can be demonstrated by the calculated Wiberg bond indices for the B–B bonds, which decrease going from B_2neop_2 (1.05) to $(Me_2Im)\cdot B_2neop_2$ (0.97) to $(Me_2Im)_2\cdot B_2neop_2$ (0.85, Fig. 3c). Our EPR data for **1a** are in accordance with those previously reported for NHC–$BH_2^{\bullet}$ radicals.[20,22,24] The structure of NHC–$BR_2^{\bullet}$ radical Me_2Im–$Bneop^{\bullet}$ and its spin density distribution were computed by DFT calculations (Fig. 2b). The NHC-boryl radical is nearly planar with the spin density delocalized between the boron atom and the NHC ring.

To verify that the EPR signal detected arose from a species preceding the RER of **1**, we monitored the reaction by VT ^1H and $^{11}B\{^1H\}$ NMR spectroscopy (Fig. 3). While the ^1H NMR spectra show broad signals as expected, the presence of the bis-NHC adduct $(Me_2Im^{Me})_2\cdot B_2neop_2$ **1** at low temperatures and the onset of the ring expansion reaction at 16 °C were easy followed by $^{11}B\{^1H\}$ NMR (Fig. 3). Below 5 °C, no signal was detected, due to the poor solubility of the starting materials. Upon warming to 5 °C, a broad signal for the bis-NHC adduct **1** was detected at 5.12 ppm, which is significantly shifted upfield from that of free B_2neop_2 (28.4 ppm),[37] as a result of rehybridization at boron from sp^2 to sp^3.

At 16 °C, the signals for the ring-expanded product RER-$(Me_2Im^{Me})_2\cdot B_2neop_2$ **2** began to arise at 1.83 and −1.35 ppm. The reaction was complete within 90 min. This observation, *i.e.*, that the RER began at the same temperature (16 °C) according to NMR spectroscopy as the EPR resonance was observed at (16.9 °C), supports the assumption that the EPR signal detected

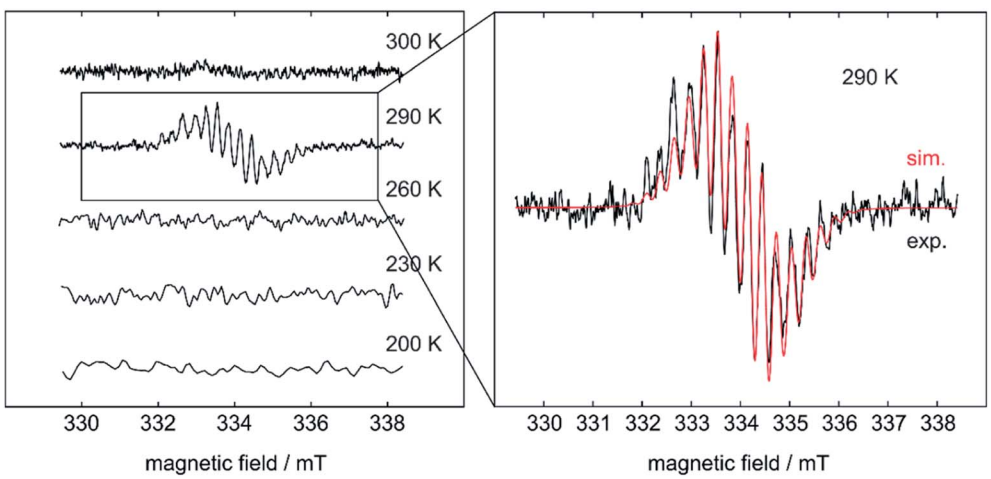

Fig. 1 Simulated (red) and experimental (black) EPR spectrum of the RER of B_2neop_2 with two equivalents Me_2Im^{Me} in THF.

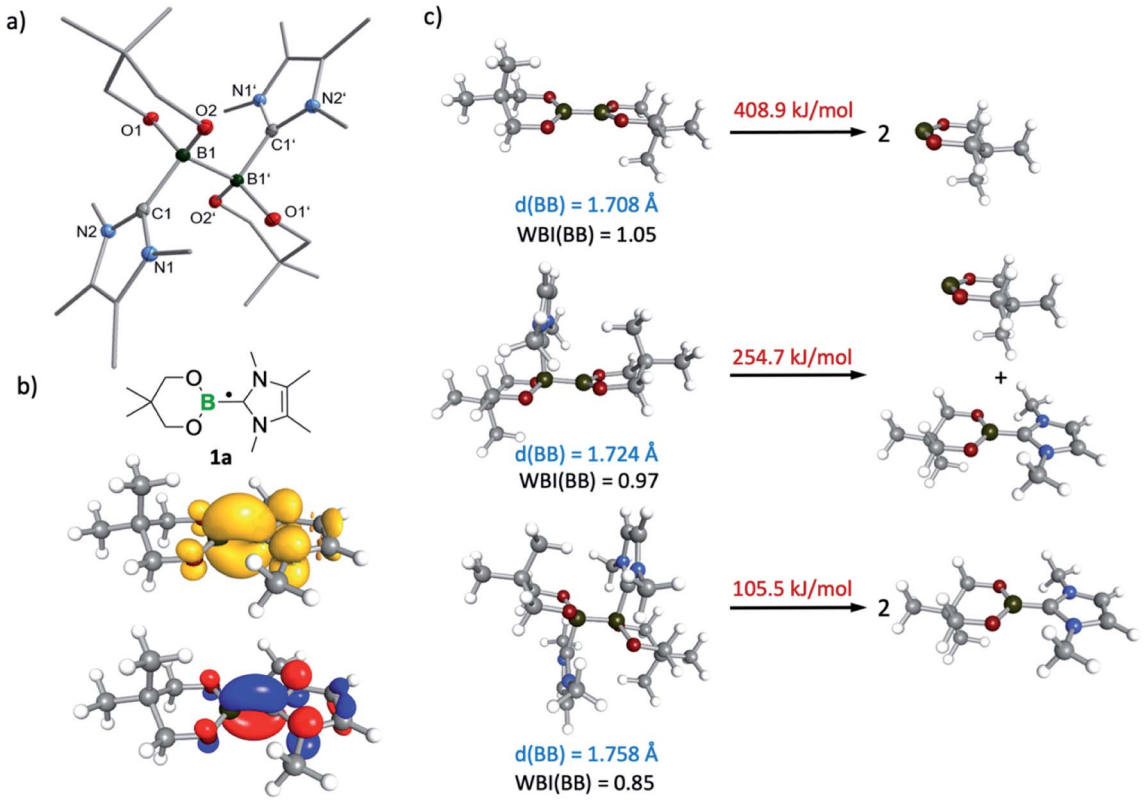

Fig. 2 (a) Molecular structure of $(Me_2Im^{Me})_2 \cdot B_2neop_2$ **1**. Hydrogen atoms are omitted for clarity and the thermal ellipsoids are drawn at 50% probability. Selected bond lengths [Å] and angles [°]: B1–B1′ 1.770(2), B1–C1 1.662(2), B1–O1 1.482(1), B1–O2 1.486(1), C1–B1–O1 109.82(8), C1–B1–O2 110.13(8). (b) Schematic structure of the NHC–$BR_2^{\bullet}$ radical **1a** (top) and the DFT-calculated (M06-2x//def2-TZVPP(B)/def2-TZVP) spin density (middle) and SOMO (bottom) for the $(Me_2Im) \cdot Bneop^{\bullet}$ radical. (c) DFT computed (M06-2x//def2-TZVPP(B)/def2-TZVP) B–B bond lengths (blue), B–B Wiberg bond indices (black) and B–B dissociation energies (red) for B_2neop_2, $(Me_2Im) \cdot B_2neop_2$ and $(Me_2Im)_2 \cdot B_2neop_2$.

is derived from a species which proceeds the RER. Another NMR spectrum recorded after 4 h at room temperature revealed that **2** had already started to decompose, which is in accordance with our previous observations.[35c]

Following studies by Stephan *et al.* on the reactivity of a doubly base-stabilized diboron(4) compound, which undergoes homolytic cleavage of the weakened B–B bond,[38] we sought to provide experimental evidence for our *in situ* observed NHC–$BR_2^{\bullet}$ moiety **1a**. Therefore, we tried to trap **1a** at temperatures below the onset of the RER, as well as during the RER process, with common radical scavengers including TEMPO ((2,2,6,6-tetramethylpiperidin-1-yl)oxyl), *N-tert*-butyl-α-phenylnitrone, diphenyl disulfide, and sulfur. However, these attempts were unsuccessful as the intramolecular RER predominated. Based on the work of Curran, Lacôte, and Lalevée on radical polymerization reactions,[26] we then employed radical **1a** as an initiator for the polymerization of styrene. Therefore, 5.0 wt% of the diboron(4) compound and two equivalents of the NHC were combined in precooled (0 °C) styrene, which was used as the solvent. The reaction mixture was allowed to warm slowly to room temperature and was stirred for 16 h. Upon adding an excess of methanol, a colorless precipitate formed, which was identified as polystyrene by size exclusion chromatography (SEC) analysis (Fig. 4). The number-average molecular weight (M_n) of the polystyrene formed was determined to 8540 Da, with a dispersity ($Đ$) of 1.74. The analogous reaction using only the diboron(4) compound (without the NHC) did not lead to the formation of polystyrene. Thus, we confirmed experimentally the formation of radical **1a** as it successfully initiated the polymerization of styrene giving polystyrene with 90% conversion.

Attempts to apply the boryl radical **1a** in metal-free borylation reactions of aryl iodides failed. The ring-expanded product **2** and the unreacted substrate employed were always obtained. Given that the NHC-boryl radical arising from the homolytic scission of **1a** is able to add to a styrene monomer before leading to **2**, it is likely that an sp^2 boron is required for the metal-free borylation to proceed.

To probe this issue, we thus investigated diboron(4) compounds with only one boron atom coordinated by an NHC (sp^2–sp^3 adducts). The B–B bond in these compounds is less activated, making them stable towards RER (with the exception of $Dipp_2Sim \cdot B_2cat_2$ at elevated temperatures[35c]). As the corresponding mono-NHC adduct $Me_2Im^{Me} \cdot B_2neop_2$, however, is not stable and begins to decompose during its preparation,[39] we synthesized the mono-NHC adduct $Me_2Im^{Me} \cdot B_2pin_2$ **3** in 73% yield using B_2pin_2 as the diboron(4) compound. Compound **3**

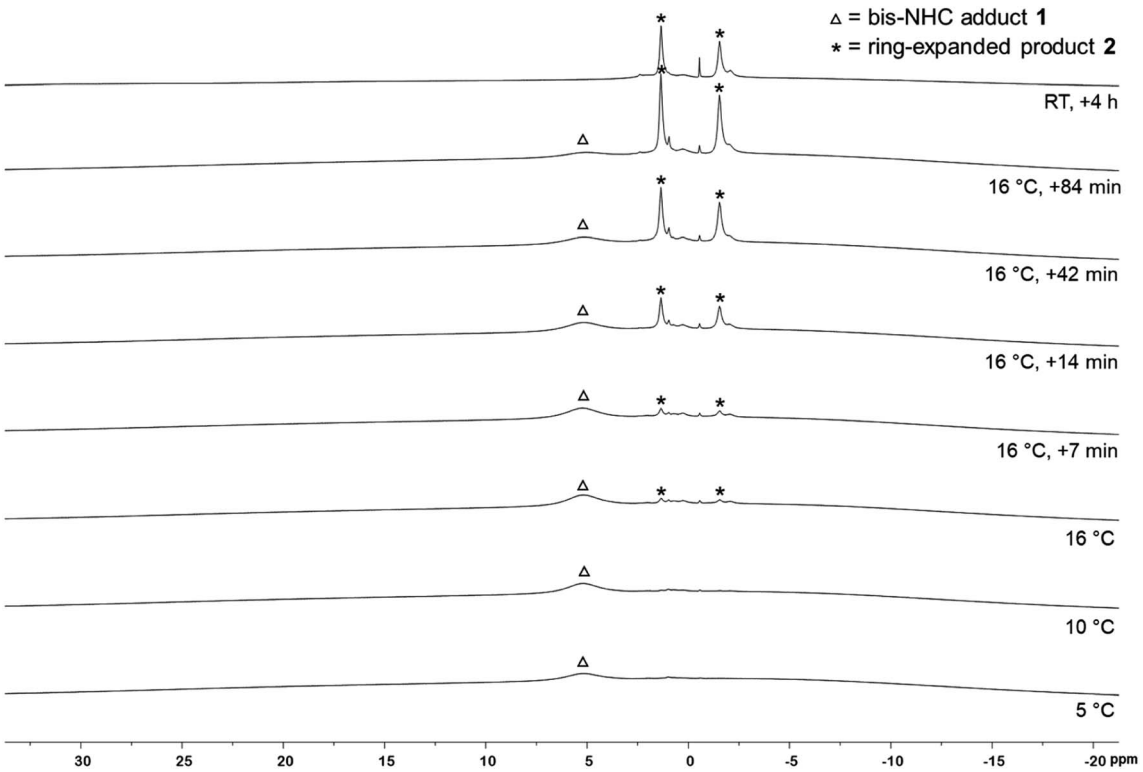

Fig. 3 ^{11}B VT-NMR spectra of the RER of B_2neop_2 with two equivalents Me_2Im^{Me} in d_8-THF (160 MHz). Triangle: bis-NHC adduct $(Me_2Im^{Me})_2{\cdot}B_2neop_2$ **1**. Asterisk: ring-expanded product RER-$(Me_2Im^{Me})_2{\cdot}B_2neop_2$ **2**.

was characterized by NMR spectroscopy, HRMS, and elemental analysis.

To study a possible transfer of one boryl moiety of a mono-NHC adduct to aryl iodides, adduct **3** was treated stoichiometrically with 4-iodotoluene **4I** (Scheme 3) in C_6D_6 and the reaction was monitored *via* ^{1}H NMR spectroscopy. At 80 °C, the first new signals appeared within 1 h, whereas full conversion of **4I** was achieved after the addition of 2.5 equivalents of **3**. The new signals match those reported for the desired C–I bond borylated product **4a**,[40] which was additionally verified by GC/MS and HRMS. Interestingly, the C–C coupling product of the aryl halide with the solvent C_6D_6 was detected as a byproduct **4b** in 25% yield (Scheme 3). Compound **4b**, as well as the analogous coupling product **4b-H**, which was obtained by running the reaction in non-deuterated benzene, were isolated and characterized *via* NMR spectroscopy, GC/MS, and HRMS.

Further reactivity studies were conducted for the reaction of **3** with different *para*-substituted aryl iodides, bromides, and chlorides (Scheme 3). Full conversion was achieved for the aryl iodides **4I–6I** and aryl bromides **4Br** and **5Br**. The ratio of the

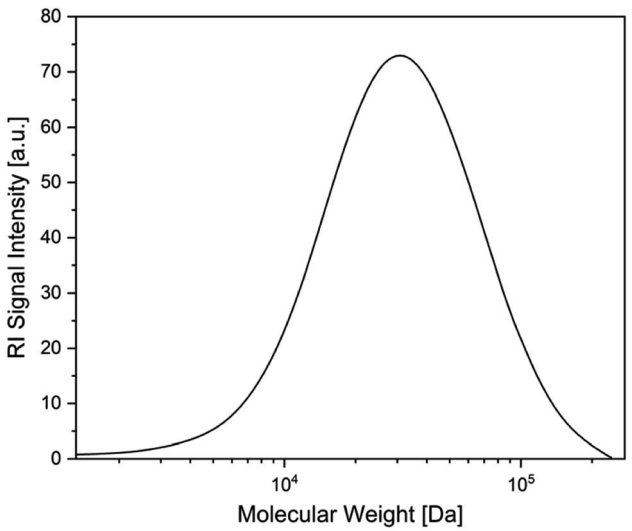

Fig. 4 Size exclusion chromatography (SEC) analysis of polystyrene.

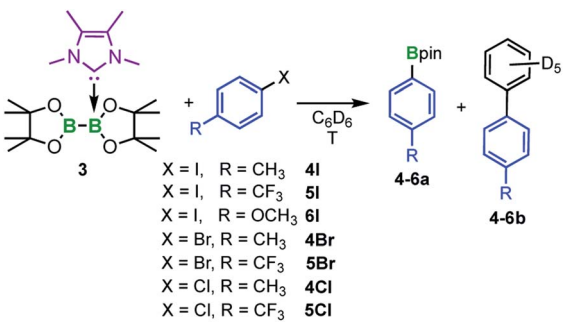

Scheme 3 Reaction of the mono-NHC adduct $Me_2Im^{Me}{\cdot}B_2pin_2$ **3** with aryl halides (X = I, Br, Cl) forming the corresponding C–X bond borylation products **4–6a** and the C–C coupling products **4–6b** between the substrate and the solvent C_6D_6.

Table 1 Reaction of the mono-NHC adduct $Me_2Im^{Me}\cdot B_2pin_2$ **3** with the aryl halides **4I–6I**, **4Br**, **5Br**, and **4Cl**, **5Cl** in C_6D_6[a]

Entry	R	T [°C]	**4–6a** [%]	**4–6b** [%]
1	CH_3 **4I**	80	75	25
2	CH_3 **4I**	50	93 (85)	7
3	CF_3 **5I**[b]	80	44[c]	56
4	CF_3 **5I**[b]	50	55[c] (44)	45
5	OCH_3 **6I**	80	80	20
6	OCH_3 **6I**	50	91(82)	9
7	CH_3 **4Br**	80	73	27
8	CH_3 **4Br**	50	92 (86)	8
9	CF_3 **5Br**[b]	80	28[c]	72
10	CF_3 **5Br**[b]	50	70[c]	30
11	CH_3 **4Cl**	80	Trace	Trace
12	CF_3 **5Cl**	80	20	12

[a] Reaction conditions: 1.0 equivalent of the aryl halide, 2.5 equivalents of **3**, C_6D_6; yields were determined *via* quantitative ^{1}H NMR spectroscopy, as well as GC/MS using biphenyl as an internal standard. Isolated yields in parentheses. [b] 3.0 equivalents of **3**. [c] In solution, the boron atom is coordinated by Me_2Im^{Me} forming the NHC adduct **5a-ADD**.

borylated arene and the C–C coupling side product strongly depends on the reaction temperature (Table 1). Lower temperatures (50 °C) diminish the formation of the byproduct from 25% to 7% (*cf.* Table 1, entries 1 and 2), but also decrease the reaction rate. For example, in the case of 4-iodobenzotrifluoride **5I**, starting material was no longer detectable after 1.5 h at 80 °C, whereas at a reaction temperature of 50 °C, full conversion was achieved only after 16 h (Fig. 5). For **5I** and **5Br**, the borylated arene was obtained in solution in the form of its Me_2Im^{Me} adduct (4-F_3C–C_6H_4-Bpin·Me_2Im^{Me} **5a-ADD**), possibly due to the more Lewis acidic boron atom resulting from the electron-withdrawing CF_3-substituent. This observation explains why an additional 0.5 equivalents of $Me_2Im^{Me}\cdot B_2pin_2$ **3** are required for full conversion of **5I** and **5Br**. For comparison, **5a-ADD** was independently synthesized and isolated (for details see ESI†).

For substrate **5I**, the reaction also proceeds slowly at room temperature, with 84% conversion after one week, and a **5a**/**b** ratio of 2 : 1. The absence of light did not have any impact on the reaction outcome. For aryl chlorides, no reaction occurred at temperatures of 50 °C. The reaction of the aryl chloride **4Cl** led to traces of **4a** at 80 °C, whereas for the more activated aryl chloride **5Cl**, 20% of the aryl boronic ester **5a** and 12% of the coupling product **5b** were observed at 80 °C (Table 1, entries 11–12). The aryl boronic esters were isolated and characterized by NMR spectroscopy, GC/MS, and HRMS.

Attempts to suppress the C–C coupling side product by performing the reaction in MTBE (methyl *tert*-butyl ether) instead of benzene, not providing any aromatic C–H bonds in the solvent, resulted in hydrodehalogenation of the aryl halide.

We then analyzed the reaction mixture of the completed reaction of **3** with **5I** by NMR spectroscopy and GC/MS. Besides the aryl boronic ester **5a** and the C–C coupling product **5b**, of **5I** with C_6D_6, residual B_2pin_2 was detected in solution. The precipitate that formed during the reaction was redissolved in chloroform and analyzed by GC/MS and NMR spectroscopy. While the GC/MS only showed traces of **5a** and B_2pin_2, ^{1}H NMR spectroscopy additionally revealed the formation of two other

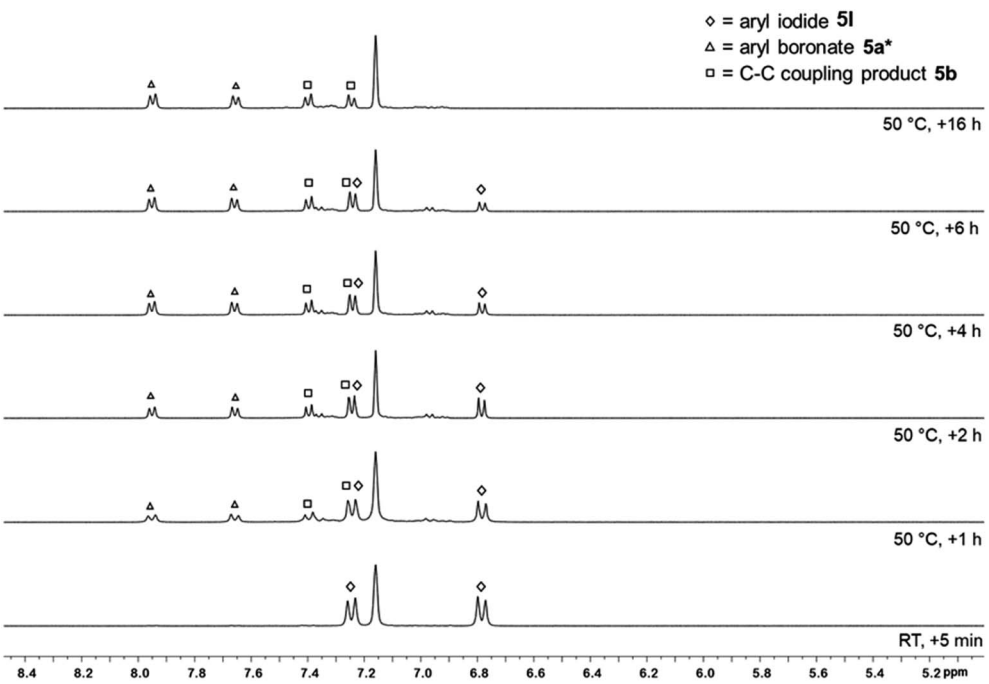

Fig. 5 *In situ* ^{1}H NMR spectra (aromatic region) of the reaction of the mono-NHC adduct $Me_2Im^{Me}\cdot B_2pin_2$ **3** and 4-iodo-benzotrifluoride **5I** in C_6D_6 at 50 °C (400 MHz). Diamond: 4-iodobenzotrifluoride **5**. Triangle: aryl boronic ester **5a** (* in solution, the boron atom is coordinated by Me_2Im^{Me} forming the NHC adduct **5a-ADD**). Square: C–C coupling product **5b**.

species (see ESI, Fig. S1†), possibly of an ionic nature, as they were not detectable by GC/MS. In the corresponding $^{11}B\{^1H\}$ NMR spectrum, besides B_2pin_2, only one significant signal was observed with a chemical shift of 1.77 ppm which, together with HRMS, and X-ray diffraction analysis (Fig. 6) was assigned to the boronium cation $[(Me_2Im^{Me})_2\cdot Bpin]^+$ **7** with iodide as the counterion. This compound might demonstrate the fate of the second boryl moiety in our boryl transfer reaction based on the mono-NHC adduct **3** (see below). The amount of **7** formed is, according to the amount of isolated residue and estimation of the ratio of **7** to the unknown species, *vide infra*, in the ^1H NMR spectrum, appropriate for it being formed stoichiometrically during the generation of the borylated arene. Thus, the formation of **7** as only a minor side product can be excluded.

The boron atom in $[(Me_2Im^{Me})_2\cdot Bpin]^+I^-$ **7** is four-coordinate, bound to the pinacolato unit and the two NHCs as σ-donating ligands, with a B–C1 bond distance of 1.663(4) Å. The data obtained match those previously reported for boronium ions.[41]

As, for the bis-NHC adduct $(Me_2Im^{Me})_2\cdot B_2neop_2$ **1**, we observed homolytic bond cleavage forming radical **1a**, we then started preliminary mechanistic investigations to determine how this boryl transfer from the mono-NHC adduct **3** to the aryl halide proceeds, and whether boryl radicals might be involved.

The C–C coupling with the solvent, as well as the observed hydrodehalogenation, are preliminary indications that aryl radicals are formed from the aryl halides.[42] The cyclic voltammograms (CV) of 4-iodotoluene **4I**, and Me_2Im^{Me} were measured in THF (for details see ESI, Fig. S4†). The redox potentials are given *versus* Ag/Ag^+ instead of Fc/Fc^+, as the free NHC reacts with Fc^+ and THF resulting in the imidazolium salt.[43] For **4I**, an irreversible reduction was observed at $E_c = -2.63$ V, showing a high electrochemical stability with respect to the acceptance of an electron. An irreversible oxidation for Me_2Im^{Me} was detected at $E_a = -1.17$ V and its reduction potential is $E_c = -2.99$ V. Thus, the formation of an aryl radical by reduction of the aryl iodide **4** by electron transfer from the free NHC can be excluded by comparing their respective potentials. However, it is conceivable that some NHCs can dimerize, leading to a tetra-amino alkene. These molecules are super electron donors, capable of generating radicals from aryl halides.[44] Therefore, free NHCs are potentially conducive to the formation of radicals in the presence of aryl halides. The feasibility of this type of radical generation was corroborated by the fact that 1 : 1 mixture of 4-iodotoluene or 4-bromotoluene, respectively, and the NHC (5.0 wt% each) lead to polymerization of styrene (see ESI†).

Moreover, the reaction of **4I** with stoichiometric amounts of the free NHC in the absence of B_2pin_2 in benzene at 80 °C also generated the C–C coupling product **4b-H** in 26% isolated yield (Scheme 4). The precipitate that was formed during the reaction was identified as the imidazolium salt $[4\text{-}CH_3\text{-}Ph\text{-}Me_2Im^{Me}]^+I^-$ **8**, characterized by GC/MS (detected as $m/z = 200$ $[M\text{-}CH_3I]^+$), HRMS and NMR spectroscopy. Besides the imidazolium salt, another, thus far unidentified, species is formed as a side product (Scheme 4). Compound **8** was not detected in the residue of the reaction mixture of the analogous reaction in the presence of B_2pin_2.

The signals of the second species detected in the ^1H NMR spectrum (Fig. 7) at a chemical shift of 2.24 and 3.86 ppm (indicated by squares), match those set of signals found in the ^1H NMR spectrum recorded of the residue formed during the boryl transfer reaction (2.24 and 3.88 ppm; *cf.* Fig. S1†). Thus, as this compound is also generated in the absence of boron and does not show any resonances in the aromatic region, it presumably must be formed from Me_2Im^{Me}. The most obvious assumption is that the signals arise from the imidazolium salt $[Me_2Im^{Me}H]^+I^-$, generated by protonation of the free NHC during the coupling of **4I** with benzene, as two singlets are detected in the expected region for the CH_3 protons of the backbone (2.24 ppm) and the NCH_3 protons (3.86 ppm) in a 1 : 1 ratio. However, no signal is detected for the C*H* proton at the former carbene carbon atom, and comparison of the signals with those of previously prepared $[Me_2Im^{Me}H]^+I^-$ (recorded in $CDCl_3$) also disproves this assumption (2.20 and 3.81 ppm). The possibility of residual free NHC in the residue reacting with $CDCl_3$ forming the analogous imidazolium salt $[Me_2Im^{Me}D]^+Cl^-$ was also excluded by a control experiment (2.14 and 3.78 ppm).

When the reaction shown in Scheme 4 was performed in the presence of stoichiometric amounts of the radical scavenger TEMPO, trace amounts of the coupling product aryl-TEMPO were detected by GC/MS, which provides further evidence for the existence of aryl radicals. The same coupling product between the aryl radical and TEMPO was observed in larger amounts by running our standard boryl transfer reaction using $Me_2Im^{Me}\cdot B_2pin_2$ **3** and 4-iodobenzotrifluoride **5I** in the presence of TEMPO (for details see ESI, Fig. S5†); however, there was no evidence for trapping of a boryl moiety.

The CV of the mono-NHC adduct **3** reveals an irreversible oxidation at $E_a = -1.17$ V, and a second one at $E_a = -0.08$ V. The former potential is identical with that observed for the free NHC. DFT calculations by the groups of Marder and Lin[6c] showed that during the exchange of the NHC between the two boron atoms in a mono-NHC adduct, no transition state could be located for an intramolecular process. Instead, a dissociation–reassociation mechanism was suggested by their theoretical studies. Thus, it is

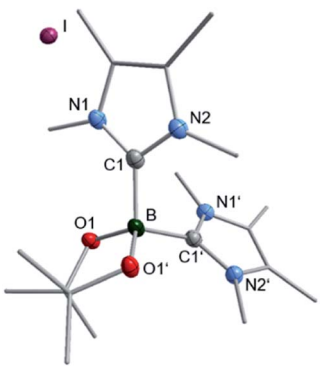

Fig. 6 Molecular structure of $[(Me_2Im^{Me})_2\cdot Bpin]^+I^-$ **7**. Hydrogen atoms are omitted for clarity and thermal ellipsoids are drawn at 50% probability. Selected bond lengths [Å] and angles [°]: B–C1 1.663(4), B–O1 1.471(3), C1–B–O1 110.80(12), C1–B–O1′ 111.23(12), C1–B1–C1′ 106.9(3).

suggested that some Me_2Im^{Me} can dissociate from B_2pin_2 in **3**, which explains the CV. In all cases, it is unlikely that **3** serves as a single electron transfer reagent.

We next ran a reaction with only B_2pin_2 and 4-iodotoluene (1 : 1 ratio) **4I** under our standard conditions. As expected, after 16 h at 80 °C, only starting materials were detected, which excludes the possibility of radicals generated by the diboron(4) compound and traces of oxygen.[45] When 0.5 equivalents of NHC were added, *ca.* 12% conversion was obtained. Upon adding another 1.5 equivalents of B_2pin_2 to the reaction mixture to accommodate the need for 2.5 equivalents in our standard reaction, no further reaction progress was observed. The subsequent addition of another 0.5 equivalents of NHC resulted in 30% conversion, revealing that the NHC does not serve as a catalyst and is required in stoichiometric amounts, therefore doing more than just initiating the reaction. The need for 2.5 equivalents of B_2pin_2 is also required as, with smaller amounts, more of the C–C coupling side product **4b** is generated. In general, the reaction also proceeds when B_2pin_2 and Me_2Im^{Me} are added separately to the reaction mixture but shows slightly increased conversion when the pre-prepared mono-NHC adduct $Me_2Im^{Me}\cdot B_2pin_2$ **3** is employed.

We then attempted the polymerization of styrene (as the solvent) at 80 °C using $Me_2Im^{Me}\cdot B_2pin_2$ **3** and 4-iodobenzotrifluoride **5I** to see whether polystyrene is formed, which would provide further experimental proof for the presence of radicals over the course of our reaction. GPC analysis (for details see ESI, Fig. S6†) confirmed the formation of polystyrene; however, with a higher number-average molecular weight (M_n) of 25 870 Da and a $Đ$ of 4.15 than that observed in the lower temperature reaction, *vide supra*, initiated by **1a**. The higher dispersity shows that there are likely many more initiation and termination steps at play. Therefore, the aryl radical is likely not the only radical species present, also providing circumstantial evidence for the presence of NHC-boryl radicals. The longer polymer chain indicates that there are likely less radicals generated which lead to fruitful initiations.

Our previous observations with 4-iodobenzotrifluoride **5I** revealed that the boryl transfer proceeds slowly at room temperature (which is not the case for the other aryl iodides), thus prompting us to monitor the reaction by EPR spectroscopy.

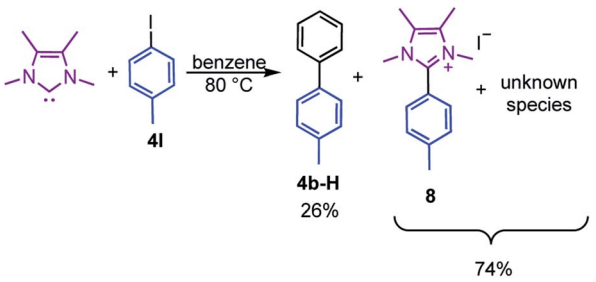

Scheme 4 Reaction of the free NHC Me_2Im^{Me} with 4-iodotoluene **4I** at 80 °C forming the C–C coupling product with the solvent **4b-H**, the imidazolium salt $[4\text{-}CH_3\text{-}Ph\text{-}Me_2Im^{Me}]^+I^-$ **8**, and an unknown compound.

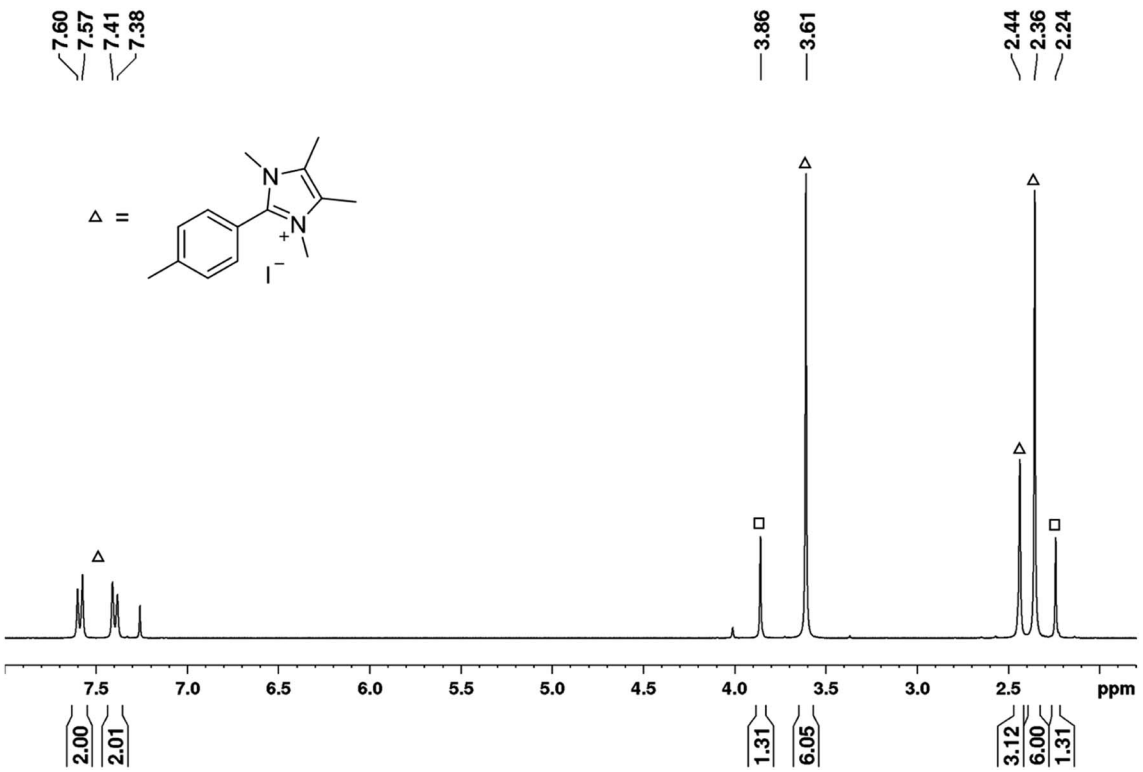

Fig. 7 ^1H NMR spectrum recorded in $CDCl_3$ (400 MHz) of the residue formed in the reaction of stoichiometric amounts of the free NHC with 4-iodotoluene **4I** showing the imidazolium salt $[4\text{-}CH_3\text{-}C_6H_4\text{–}Me_2Im^{Me}]^+I^-$ **8**, and an unknown compound (square).

An EPR signal was detected; however, due to the very slow reaction progress at room temperature, it was very weak and ill-defined. Thus, the determination of hyperfine couplings and, hence, insight into the nature of the radical was precluded. Nonetheless, the isotropic *g*-value of 2.006, together with the broad linewidth, suggest the presence of a boron-based radical (for details see ESI, Fig. S7†).

All of the data presented lead us to propose a mechanism for the metal-free borylation process (Scheme 5).

A small fraction of mono-adduct **3** is likely able to release the NHC, which ends up dimerizing. As soon as this happens, SET can occur with the aryl halide, which starts the radical chain reaction (initiation step, (1) in Scheme 5). Once the aryl radical is formed it can add to the sp^2 boron of **3** (which explains why **1** does not lead to borylation of aryl halides). The B–B bond undergoes homolytic scission, presumably in a single elementary step **A** (homolytic substitution at boron), or *via* some associative mechanism (radical addition followed by radical release). In both cases, this delivers the borylated product as well as an NHC-boryl radical (**B**), which is stabilized by partial delocalization of the spin. **B** can then proceed to abstract the halogen atom from aryl halide **4**, thus closing the radical chain. Alternatively, the aryl radicals can also react with the solvent, leading to the biaryls observed. We did not try to optimize this further as our focus was on the fate of the diboron compound, but the insights obtained may prove useful to develop an alternative to the pyridine-based metal-free borylations.

After termination, the desired arylboronate product can intercept the NHC, provided the Lewis acidity of the product is high enough (as is the case for the reactions of Table 1, entries 9–10). Finally, the boron byproduct **C** can also react with the NHC, which leads to boronium ion **7** (Fig. 6). The higher Lewis basicity of the carbenes compared with pyridines prevents the catalytic turnover of the Lewis base, which allowed us to isolate the key byproduct **7**.

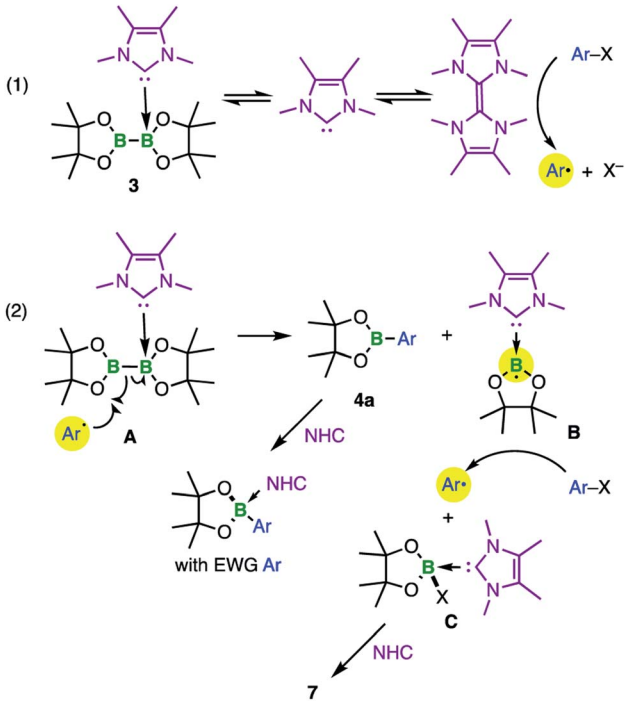

Scheme 5 Proposed mechanism for the borylation of aryl halides.

Conclusions

Former studies by the groups of Marder and Radius have shown that bis-NHC adducts of diboron(4) compounds are thermally unstable, undergoing ring expansion reactions (RER) *via* the insertion of one $B(OR)_2$ moiety into the C–N bond of one NHC with the second $B(OR)_2$ moiety bound *exo* to the former carbene–carbon atom.[35] Based on these findings, the reaction of B_2neop_2 with two equivalents of Me_2Im^{Me} was followed by ^{11}B NMR spectroscopy revealing that, at low temperatures, the bis-NHC adduct $(Me_2Im^{Me})_2{\cdot}B_2neop_2$ **1** is formed which, at 16 °C, starts undergoing a ring expansion reaction. Monitoring the same reaction by EPR spectroscopy provided evidence for the RER proceeding *via* the formation of a boryl radical of the type $NHC–BR_2^{\bullet}$ **1a**, presumably formed by homolytic B–B bond cleavage. Radical **1a** was successfully applied as an initiator for the radical polymerization of styrene. Further investigations with respect to applying the boryl moiety **1a** in a metal-free borylation reaction by suppressing the RER failed. Therefore, the mono-NHC adduct $Me_2Im^{Me}{\cdot}B_2pin_2$ **3** was synthesized. Because it is a mono-adduct, its B–B bond is less activated and therefore stable towards RER. The stoichiometric reaction of **3** with different substituted aryl iodides and bromides in benzene, at elevated temperatures, led to boryl transfer and gave the desired aryl boronic esters in good yields. Interestingly, varying amounts of a C–C coupling product between the aryl halide and the solvent (benzene), depending on the reaction temperature, were detected as a side product. Further studies concerning the mechanism of this boryl transfer reaction revealed that radicals are likely involved, as an aryl radical was trapped by TEMPO, and running the boryl transfer reaction in styrene led to its polymerization. Monitoring the reaction by EPR spectroscopy revealed a signal (though very weak and ill-defined), which is suggestive of a boron-based radical. Furthermore, the boronium cation $[(Me_2Im^{Me})_2{\cdot}Bpin]^+I^-$ **7** was formed stoichiometrically during the boryl transfer reaction, possibly demonstrating the fate of the second boryl moiety. NHCs are beneficial when strong complexation (and simultaneous homolytic cleavage of the B–B bond) is needed, as is the case for initiation of radical polymerizations, or stabilization of crucial intermediates in the metal-free borylation. Further work will focus on the development of safe, low-temperature initiators for radical polymerizations (in contrast to, *e.g.*, azo initiators which decompose at room temperature, and are intrinsically dangerous) as the bis-adducts could be assembled within the polymerization vessel only when needed.

Data availability

Additional data and spectra, and crystallographic data, NMR spectra, and Cartesian coordinates for calculations can be found in the ESI.†

Author contributions

All authors contributed to research, writing, and editing of the article. E. L., T. B. M. and U. R. designed the project; L. K., L. Z., L. W., M. S. and S. W.-P. designed and performed the experiments; L. K., L. W. and U. R. performed the XRD studies, U. R. designed and performed the computational studies; H. B. and I. K. designed and performed the EPR studies; L. Z. performed CV studies; L. K., E. L., T. B. M. and U. R. wrote the manuscript with input from all the other co-authors.

Conflicts of interest

There are no conflicts of interest to declare.

Acknowledgements

This work was supported by funds from the Julius-Maximilians-Universität Würzburg and the Deutsche Forschungsgemeinschaft (DFG). We thank AllyChem Co. Ltd. for a generous gift of diboron(4) reagents and Johanna Lutz for the GPC measurements. E. L. thanks the Alexander von Humboldt Foundation for a Bessel Award.

References

1 (*a*) D. G. Hall, *Boronic Acids: Preparation and Applications in Organic Synthesis, Medicine and Materials*, ed. D. G. Hall, Wiley-VCH, Weinheim, 2nd edn, 2011; (*b*) E. C. Neeve, S. J. Geier, I. A. I. Mkhalid, S. A. Westcott and T. B. Marder, *Chem. Rev.*, 2016, **116**, 9091–9161.

2 (*a*) N. Miyaura, T. Yanagi and A. Suzuki, *Synth. Commun.*, 1981, **11**, 513–519; (*b*) N. Miyaura and A. Suzuki, *Chem. Rev.*, 1995, **95**, 2457–2483.

3 (*a*) C. Kleeberg, L. Dang, Z. Lin and T. B. Marder, *Angew. Chem., Int. Ed.*, 2009, **48**, 5350–5354; (*b*) S. K. Bose, K. Fucke, L. Liu, P. G. Steel and T. B. Marder, *Angew. Chem., Int. Ed.*, 2014, **53**, 1799–1803; (*c*) S. K. Bose, A. Deißenberger, A. Eichhorn, P. G. Steel, Z. Lin and T. B. Marder, *Angew. Chem., Int. Ed.*, 2015, **54**, 11843–11847; (*d*) J. Zhou, M. W. Kuntze-Fechner, R. Bertermann, U. S. D. Paul, J. H. J. Berthel, A. Friedrich, Z. Du, T. B. Marder and U. Radius, *J. Am. Chem. Soc.*, 2016, **138**, 5250–5253; (*e*) S. K. Bose, S. Brand, H. O. Omoregie, M. Haehnel, J. Maier, G. Bringmann and T. B. Marder, *ACS Catal.*, 2016, **6**, 8332–8335; (*f*) Y.-M. Tian, X.-N. Guo, M. W. Kuntze-Fechner, I. Krummenacher, H. Braunschweig, U. Radius, A. Steffen and T. B. Marder, *J. Am. Chem. Soc.*, 2018, **140**, 17612–17623; (*g*) L. Kuehn, M. Huang, U. Radius and T. B. Marder, *Org. Biomol. Chem.*, 2019, **17**, 6601–6606; (*h*) L. Kuehn, D. G. Jammal, K. Lubitz, T. B. Marder and U. Radius, *Chem.–Eur. J.*, 2019, **25**, 9514–9521; (*i*) Y.-M. Tian, X.-N. Guo, Z. Wu, A. Friedrich, S. A. Westcott, H. Braunschweig, U. Radius and T. B. Marder, *J. Am. Chem. Soc.*, 2020, **142**, 13136–13144; (*j*) Y.-M. Tian, X.-N. Guo, I. Krummenacher, Z. Wu, J. Nitsch, H. Braunschweig, U. Radius and T. B. Marder, *J. Am. Chem. Soc.*, 2020, **142**, 18231–18242; (*k*) M. Huang, Z. Wu, J. Krebs, A. Friedrich, X. Luo, S. A. Westcott, U. Radius and T. B. Marder, *Chem.–Eur. J.*, 2021, **27**, 8149–8158.

4 (*a*) V. Lillo, A. Bonet and E. Fernández, *Dalton Trans.*, 2009, 2899–2908; (*b*) K. Semba, T. Fujihara, J. Terao and Y. Tsuji, *Tetrahedron*, 2015, **71**, 2183–2197; (*c*) V. Ritleng, M. Henrion and M. J. Chetcuti, *ACS Catal.*, 2016, **6**, 890–906; (*d*) K. Kubota, H. Iwamoto and H. Ito, *Org. Biomol. Chem.*, 2017, **15**, 285–300; (*e*) H. Yoshida, *ACS Catal.*, 2016, **6**, 1799–1811; (*f*) J. V. Obligacion and P. J. Chirik, *Nat. Rev. Chem.*, 2018, **2**, 15–34; (*g*) D. Hemming, R. Fritzemeier, S. A. Westcott, W. L. Santos and P. G. Steel, *Chem. Soc. Rev.*, 2018, **47**, 7477–7494; (*h*) S. K. Bose and T. B. Marder, *Org. Lett.*, 2014, **16**, 4562–4565; (*i*) Y.-M. Tian, X.-N. Guo, H. Braunschweig, U. Radius and T. B. Marder, *Chem. Rev.*, 2021, **121**, 3561–3597; (*j*) S. K. Bose, L. Mao, L. Kuehn, U. Radius, J. Nekvinda, W. L. Santos, S. A. Westcott, P. G. Steel and T. B. Marder, *Chem. Rev.*, 2021, **121**, 13238–13341; (*k*) J. Hu, M. Ferger, Z. Shi and T. B. Marder, *Chem. Soc. Rev.*, 2021, **50**, 13129–13188; (*l*) K. Muthuvel and T. Gandhi, *ChemCatChem*, 2022, e202101579.

5 (*a*) R. D. Dewhurst, E. C. Neeve, H. Braunschweig and T. B. Marder, *Chem. Commun.*, 2015, **51**, 9594–9607; (*b*) S. Pietsch, E. C. Neeve, D. C. Apperley, R. Bertermann, F. Mo, D. Qiu, M. S. Cheung, L. Dang, J. Wang, U. Radius, Z. Lin, C. Kleeberg and T. B. Marder, *Chem.–Eur. J.*, 2015, **21**, 7082–7098; (*c*) S. Würtemberger-Pietsch, U. Radius and T. B. Marder, *Dalton Trans.*, 2016, **45**, 5880–5895; (*d*) A. B. Cuenca, R. Shishido, H. Ito and E. Fernández, *Chem. Soc. Rev.*, 2017, **46**, 415–430; (*e*) L. Kuehn, M. Stang, S. Würtemberger-Pietsch, A. Friedrich, H. Schneider, U. Radius and T. B. Marder, *Faraday Discuss.*, 2019, **220**, 350–363; (*f*) M. Huang, J. Hu, S. Shi, A. Friedrich, J. Krebs, S. A. Westcott, U. Radius and T. B. Marder, *Chem.–Eur. J.*, 2022, **28**, e202200480.

6 (*a*) K.-s. Lee, A. R. Zhugralin and A. H. Hoveyda, *J. Am. Chem. Soc.*, 2009, **131**, 7253–7255; (*b*) K.-s. Lee, A. R. Zhugralin and A. H. Hoveyda, *J. Am. Chem. Soc.*, 2010, **132**, 12766; (*c*) C. Kleeberg, A. G. Crawford, A. S. Batsanov, P. Hodgkinson, D. C. Apperley, M. S. Cheung, Z. Lin and T. B. Marder, *J. Org. Chem.*, 2012, **77**, 785–789.

7 (*a*) F. Mo, Y. Jiang, D. Qiu, Y. Zhang and J. Wang, *Angew. Chem., Int. Ed.*, 2010, **49**, 1846–1849; (*b*) D. Qiu, L. Jin, Z. Zheng, H. Meng, F. Mo, X. Wang, Y. Zhang and J. Wang, *J. Org. Chem.*, 2013, **78**, 1923–1933.

8 (*a*) G. Yan, D. Huang and X. Wu, *Adv. Synth. Catal.*, 2018, **360**, 1039; (*b*) F. W. Friese and A. Studer, *Chem. Sci.*, 2019, **10**, 8503–8518; (*c*) T. Taniguchi, *Eur. J. Org. Chem.*, 2019, 6308–6319; (*d*) L. Zheng, L. Cai, K. Tao, Z. Xie, Y.-L. Lai and W. Guo, *Asian J. Org. Chem.*, 2021, **10**, 711–748; (*e*) L. Qiang, Z. Lei and M. Fanyang, *Acta Chim. Sin.*, 2020, **78**, 1297–1308.

9 (*a*) K. Oshima, T. Ohmura and M. Suginome, *Chem. Commun.*, 2012, **48**, 8571–8573; (*b*) T. Ohmura, Y. Morimasa and M. Suginome, *J. Am. Chem. Soc.*, 2015, **137**, 2852–2855.

10 T. Ohmura, Y. Morimasa, T. Ichino, Y. Miyake, Y. Murata, M. Suginome, K. Tajima, T. Taketsugu and S. Maeda, *Bull. Chem. Soc. Jpn.*, 2021, **94**, 1894–1902.

11 (*a*) G. Wang, H. Zhang, J. Zhao, W. Li, J. Cao, C. Zhu and S. Li, *Angew. Chem., Int. Ed.*, 2016, **55**, 5985–5989; (*b*) G. Wang, J. Cao, L. Gao, W. Chen, W. Huang, X. Cheng and S. Li, *J. Am. Chem. Soc.*, 2017, **139**, 3904–3910; (*c*) J. Cao, G. Wang, L. Gao, X. Cheng and S. Li, *Chem. Sci.*, 2018, **9**, 3664–3671.

12 R. Xu, G.-p. Lu and C. Cai, *New J. Chem.*, 2018, **42**, 16456–16459.

13 (*a*) L. Zhang and L. Jiao, *J. Am. Chem. Soc.*, 2017, **139**, 607–610; (*b*) L. Zhang and L. Jiao, *Chem. Sci.*, 2018, **9**, 2711–2722; (*c*) L. Zhang and L. Jiao, *J. Am. Chem. Soc.*, 2019, **141**, 9124–9128.

14 S. Pinet, V. Liautard, M. Debiais and M. Pucheault, *Synthesis*, 2017, **49**, 4759–4768.

15 W.-M. Cheng, R. Shang, B. Zhao, W.-L. Xing and Y. Fu, *Org. Lett.*, 2017, **19**, 4291–4294.

16 (*a*) A. Yoshimura, Y. Takamachi, L.-B. Han and A. Ogawa, *Chem.–Eur. J.*, 2015, **21**, 13930–13933; (*b*) A. Yoshimura, Y. Takamachi, K. Mihara, T. Saeki, S.-i. Kawaguchi, L.-B. Han, A. Nomoto and A. Ogawa, *Tetrahedron*, 2016, **72**, 7832–7838.

17 (*a*) Y. Cheng, C. Mück-Lichtenfeld and A. Studer, *Angew. Chem., Int. Ed.*, 2018, **57**, 16832–16836; (*b*) Y. Cheng, C. Mück-Lichtenfeld and A. Studer, *J. Am. Chem. Soc.*, 2018, **140**, 6221–6225.

18 G. Li, G. Huang, R. Sun, D. P. Curran and W. Dai, *Org. Lett.*, 2021, **23**, 4353–4357.

19 (*a*) M. Huang, J. Hu, M. Tang, S. A. Westcott, U. Radius and T. B. Marder, *Chem. Commun.*, 2022, **58**, 395–398; (*b*) M. Huang, J. Hu, I. Krummenacher, A. Friedrich, H. Braunschweig, S. A. Westcott, U. Radius and T. B. Marder, *Chem.–Eur. J.*, 2022, **28**, e202103866.

20 (*a*) P. P. Power, *Chem. Rev.*, 2003, **103**, 789–810; (*b*) Y. Su and R. Kinjo, *Coord. Chem. Rev.*, 2017, **352**, 346–378; (*c*) T. Taniguchi, *Chem. Soc. Rev.*, 2021, 8995–9021.

21 (*a*) E. Krause and H. Polack, *Ber. Dtsch. Chem. Ges.*, 1926, **59**, 777–785; (*b*) T. L. Chu and T. J. Weismann, *J. Am. Chem. Soc.*, 1956, **78**, 23–26; (*c*) W. Kaim and A. Schulz, *Angew. Chem., Int. Ed.*, 1984, **23**, 615–616; (*d*) A. Schulz and W. Kaim, *Chem. Ber.*, 1989, **122**, 1863–1868; (*e*) L. Ji, R. M. Edkins, A. Lorbach, I. Krummenacher, C. Brückner, A. Eichhorn, H. Braunschweig, B. Engels, P. J. Low and T. B. Marder, *J. Am. Chem. Soc.*, 2015, **137**, 6750–6753; (*f*) Y. Zheng, J. Xiong, Y. Sun, X. Pan and J. Wu, *Angew. Chem., Int. Ed.*, 2015, **54**, 12933–12936; (*g*) F. Rauch, S. Fuchs, A. Friedrich, D. Sieh, I. Krummenacher, H. Braunschweig, M. Finze and T. B. Marder, *Chem.–Eur. J.*, 2020, **26**, 12794–12808; (*h*) X. Jia, J. Nitsch, Z. Wu, A. Friedrich, J. Krebs, I. Krummenacher, F. Fantuzzi, H. Braunschweig, M. Moos, C. Lambert, B. Engels and T. B. Marder, *Chem. Sci.*, 2021, **12**, 11864–11872; (*i*) J. Krebs, M. Haehnel, I. Krummenacher, A. Friedrich, H. Braunschweig, M. Finze, L. Ji and T. B. Marder, *Chem.–Eur. J.*, 2021, **27**, 8159–8167.

22 (*a*) S.-H. Ueng, M. Makhlouf Brahmi, É. Derat, L. Fensterbank, E. Lacôte, M. Malacria and D. P. Curran, *J. Am. Chem. Soc.*, 2008, **130**, 10082–10083; (*b*) S. Telitel, A.-L. Vallet, S. Schweizer, B. Delpech, N. Blanchard, F. Morlet-Savary, B. Graff, D. P. Curran, M. Robert, E. Lacôte and J. Lalevée, *J. Am. Chem. Soc.*, 2013, **135**, 16938–16947.

23 (*a*) C. D. Martin, M. Soleilhavoup and G. Bertrand, *Chem. Sci.*, 2013, **4**, 3020–3030; (*b*) S. Kundu, S. Sinhababu, V. Chandrasekhar and H. W. Roesky, *Chem. Sci.*, 2019, **10**, 4727–4741.

24 (*a*) S.-H. Ueng, A. Solovyev, X. Yuan, S. J. Geib, L. Fensterbank, E. Lacôte, M. Malacria, M. Newcomb, J. C. Walton and D. P. Curran, *J. Am. Chem. Soc.*, 2009, **131**, 11256–11262; (*b*) J. C. Walton, M. M. Brahmi, L. Fensterbank, E. Lacôte, M. Malacria, Q. Chu, S.-H. Ueng, A. Solovyev and D. P. Curran, *J. Am. Chem. Soc.*, 2010, **132**, 2350–2358.

25 (*a*) P. R. Rablen and J. F. Hartwig, *J. Am. Chem. Soc.*, 1996, **118**, 4648–4653; (*b*) P. R. Rablen, *J. Am. Chem. Soc.*, 1997, **119**, 8350–8360.

26 (*a*) D. P. Curran, A. Solovyev, M. Makhlouf Brahmi, L. Fensterbank, M. Malacria and E. Lacôte, *Angew. Chem., Int. Ed.*, 2011, **50**, 10294–10317; (*b*) M.-A. Tehfe, M. M. Brahmi, J.-P. Fouassier, D. P. Curran, M. Malacria, L. Fensterbank, E. Lacôte and J. Lalevée, *Macromolecules*, 2010, **43**, 2261–2267; (*c*) S.-H. Ueng, L. Fensterbank, E. Lacôte, M. Malacria and D. P. Curran, *Org. Lett.*, 2010, **12**, 3002–3005; (*d*) M.-A. Tehfe, J. Monot, M. M. Brahmi, H. Bonin-Dubarle, D. P. Curran, M. Malacria, L. Fensterbank, E. Lacôte, J. Lalevée and J.-P. Fouassier, *Polym. Chem.*, 2011, **2**, 625–631; (*e*) M.-A. Tehfe, J. Monot, M. Malacria, L. Fensterbank, J.-P. Fouassier, D. P. Curran, E. Lacôte and J. Lalevée, *ACS Macro Lett.*, 2012, **1**, 92–95; (*f*) J. Lalevée, S. Telitel, M. A. Tehfe, J. P. Fouassier, D. P. Curran and E. Lacôte, *Angew. Chem., Int. Ed.*, 2012, **51**, 5958–5961; (*g*) S. Telitel, S. Schweizer, F. Morlet-Savary, B. Graff, T. Tschamber, N. Blanchard, J. P. Fouassier, M. Lelli, E. Lacôte and J. Lalevée, *Macromolecules*, 2013, **46**, 43–48; (*h*) J. C. Walton, M. M. Brahmi, J. Monot, L. Fensterbank, M. Malacria, D. P. Curran and E. Lacôte, *J. Am. Chem. Soc.*, 2011, **133**, 10312–10321.

27 (*a*) T. Watanabe, D. Hirose, D. P. Curran and T. Taniguchi, *Chem.–Eur. J.*, 2017, **23**, 5404–5409; (*b*) S.-C. Ren, F.-L. Zhang, J. Qi, Y.-S. Huang, A.-Q. Xu, H.-Y. Yan and Y.-F. Wang, *J. Am. Chem. Soc.*, 2017, **139**, 6050–6053; (*c*) J. Qi, F.-L. Zhang, Y.-S. Huang, A.-Q. Xu, S.-C. Ren, Z.-Y. Yi and Y.-F. Wang, *Org. Lett.*, 2018, **20**, 2360–2364; (*d*) J.-K. Jin, F.-L. Zhang, Q. Zhao, J.-A. Lu and Y.-F. Wang, *Org. Lett.*, 2018, **20**, 7558–7562; (*e*) K. Takahashi, M. Shimoi, T. Watanabe, K. Maeda, S. J. Geib, D. P. Curran and T. Taniguchi, *Org. Lett.*, 2020, **22**, 2054–2059; (*f*) Y.-S. Huang, J. Wang, W.-X. Zheng, F.-L. Zhang, Y.-J. Yu, M. Zheng, X. Zhou and Y.-F. Wang, *Chem. Commun.*, 2019, **55**, 11904–11907.

28 For other examples, see ref. 7, 19, and 22.

29 C.-W. Chiu and F. P. Gabbaï, *Angew. Chem., Int. Ed.*, 2007, **46**, 1723–1725.
30 T. Matsumoto and F. P. Gabbaï, *Organometallics*, 2009, **28**, 4252–4253.
31 P. Bissinger, H. Braunschweig, A. Damme, I. Krummenacher, A. K. Phukan, K. Radacki and S. Sugawara, *Angew. Chem., Int. Ed.*, 2014, **53**, 7360–7363.
32 F. Dahcheh, D. Martin, D. W. Stephan and G. Bertrand, *Angew. Chem., Int. Ed.*, 2014, **53**, 13159–13163.
33 M. F. Silva Valverde, P. Schweyen, D. Gisinger, T. Bannenberg, M. Freytag, C. Kleeberg and M. Tamm, *Angew. Chem., Int. Ed.*, 2017, **56**, 1135–1140.
34 (*a*) P. Nguyen, C. Dai, N. J. Taylor, W. P. Power, T. B. Marder, N. L. Pickett and N. C. Norman, *Inorg. Chem.*, 1995, **34**, 4290–4291; (*b*) W. Clegg, C. Dai, F. J. Lawlor, T. B. Marder, P. Nguyen, N. C. Norman, N. L. Pickett, W. P. Power and A. J. Scott, *J. Chem. Soc., Dalton Trans.*, 1997, 839–846.
35 (*a*) S. Pietsch, U. Paul, I. A. Cade, M. J. Ingleson, U. Radius and T. B. Marder, *Chem.–Eur. J.*, 2015, **21**, 9018–9021; (*b*) S. Würtemberger-Pietsch, H. Schneider, T. B. Marder and U. Radius, *Chem.–Eur. J.*, 2016, **22**, 13032–13036; (*c*) M. Eck, S. Würtemberger-Pietsch, A. Eichhorn, J. H. J. Berthel, R. Bertermann, U. S. D. Paul, H. Schneider, A. Friedrich, C. Kleeberg, U. Radius and T. B. Marder, *Dalton Trans.*, 2017, **46**, 3661–3680; (*d*) A. F. Eichhorn, S. Fuchs, M. Flock, T. B. Marder and U. Radius, *Angew. Chem., Int. Ed.*, 2017, **56**, 10209–10213.
36 M. Gao, S. B. Thorpe, C. Kleeberg, C. Slebodnick, T. B. Marder and W. L. Santos, *J. Org. Chem.*, 2011, **76**, 3997–4007.
37 F. J. Lawlor, N. C. Norman, N. L. Pickett, E. G. Robins, P. Nguyen, G. Lesley, T. B. Marder, J. A. Ashmore and J. C. Green, *Inorg. Chem.*, 1998, **37**, 5282–5288.
38 L. L. Cao and D. W. Stephan, *Organometallics*, 2017, **36**, 3163–3170.
39 S. Würtemberger-Pietsch, PhD thesis, Julius-Maximilians-Universität Würzburg, 2016.
40 (*a*) M. Murata, T. Oyama, S. Watanabe and Y. Masuda, *J. Org. Chem.*, 2000, **65**, 164–168; (*b*) A. Wolan and M. Zaidlewicz, *Org. Biomol. Chem.*, 2003, **1**, 3274–3276.
41 (*a*) D. J. Brauer, H. Bürger, G. Pawelke, W. Weuter and J. Wilke, *J. Organomet. Chem.*, 1987, **329**, 293–304; (*b*) W. E. Piers, S. C. Bourke and K. D. Conroy, *Angew. Chem., Int. Ed.*, 2005, **44**, 5016–5036; (*c*) O. J. Metters, A. M. Chapman, A. P. M. Robertson, C. H. Woodall, P. J. Gates, D. F. Wass and I. Manners, *Chem. Commun.*, 2014, **50**, 12146–12149.
42 (*a*) S. Yanagisawa, K. Ueda, T. Taniguchi and K. Itami, *Org. Lett.*, 2008, **10**, 4673–4676; (*b*) G. Deng, K. Ueda, S. Yanagisawa, K. Itami and C.-J. Li, *Chem.–Eur. J.*, 2009, **15**, 333–337.
43 T. Ramnial, I. McKenzie, B. Gorodetsky, E. M. W. Tsang and J. A. C. Clyburne, *Chem. Commun.*, 2004, 1054–1055.
44 (*a*) J. A. Murphy, T. A. Khan, S.-z. Zhou, D. W. Thomson and M. Mahesh, *Angew. Chem., Int. Ed.*, 2005, **44**, 1356–1360; (*b*) J. A. Murphy, S.-z. Zhou, D. W. Thomson, F. Schoenebeck, M. Mahesh, S. R. Park, T. Tuttle and L. E. A. Berlouis, *Angew. Chem., Int. Ed.*, 2007, **46**, 5178–5183.
45 C. Ollivier and P. Renaud, *Chem. Rev.*, 2001, **101**, 3415–3434.